Marine and Petroleum Geology 114 (2020) 104231

Contents lists available at ScienceDirect

Marine and Petroleum Geology

journal homepage: www.elsevier.com/locate/marpetgeo

Research paper

The Baiyun Slide Complex, South China Sea: A modern example of slope instability controlling submarine-channel incision on continental slopes

Wei Li[a,b,c,*], Tiago M. Alves[d], Michele Rebesco[e], Jie Sun[a,b,**], Jian Li[a,c], Shuang Li[a,c], Shiguo Wu[f]

[a] CAS Key Laboratory of Ocean and Marginal Sea Geology, South China Sea Institute of Oceanology, Chinese Academy of Sciences, Guangzhou, 510301, PR China
[b] Innovation Academy of South China Sea Ecology and Environmental Engineering, Chinese Academy of Sciences, Guangzhou, 510301, PR China
[c] University of Chinese Academy of Sciences, Beijing, 100049, PR China
[d] 3D Seismic Lab. School of Earth and Ocean Sciences, Cardiff University, Main Building, Park Place, Cardiff, CF10 3AT, United Kingdom
[e] Istituto Nazionale di Oceanografia e di Geofisica Sperimentale (OGS), Borgo Grotta Gigante 42/C, Sgonico, 34010, Trieste, Italy
[f] Institute of Deep-sea Science and Engineering, Chinese Academy of Sciences, Sanya, 572000, PR China

ARTICLE INFO

Keywords:
South China Sea
Submarine landslide
Submarine channels
Bottom currents
Turbidity currents

ABSTRACT

The Baiyun Slide Complex is one of the largest submarine landslides on the northern margin of the South China Sea. Newly acquired high-resolution bathymetric data, 2D and 3D seismic data permitted the systematic investigation of the Baiyun Slide Complex in terms of its seafloor morphology and associated sedimentary processes. The headwall region of the Baiyun Slide Complex, located at a water depth between 1000 m and 1700 m, is U-shaped and opens towards the east. It was efficiently and almost completely evacuated, generating pronounced headwall and sidewall scarps. Submarine channels, sediment waves, migrating channels, sediment drifts and moats are observed within and around the headwall region, illustrating the effects of both downslope and along-slope sedimentary processes. Submarine channels are 16–37 km-long 800-1500 m-wide, and 20 to 50 m-deep. As a modern example of the interplay between slope instability and subsequent incision, submarine channels were generated after the formation of the Baiyun Slide scar to suggest intensified downslope sedimentary processes after the slope collapsed. The initiation and formation of these submarine channels result from the evacuation of the Baiyun Slide scar, which provided the necessary space of the continental slope to accommodate subsequent turbidity and mass wasting flows. Our results are an important example of how submarine landslides can influence erosional and depositional processes on continental margins.

1. Introduction

Submarine landslides, turbidity currents and bottom currents are dominant sedimentary processes occurring along both passive and active continental margins (Vorren et al., 1998; Rebesco et al., 2014; Mosher et al., 2017). Downslope processes such as landslides and turbidity currents are driven by gravity and lead to the deposition of broad mass-transport deposits or turbidite systems within erosive channels (Moscardelli et al., 2006; Casalbore et al., 2010; Bourget et al., 2011; Li et al., 2015b). They can transport large volumes (> 100 km^3) of sediment sourced from the continental shelf and upper slope areas into the deep ocean (Georgiopoulou et al., 2010; Li et al., 2018), re-shaping the sea floor to influence subsequent sedimentary processes (Casalbore et al., 2018). They can also control the distribution of sand in deep-water environments (Haflidason et al., 2004; Mosher et al., 2017). Along-slope bottom currents result in extensive depositional (e.g. sediment drifts) and erosional (e.g. contourite channels) features on outer continental shelves and upper continental slopes (Hernández-Molina et al., 2006; García et al., 2009; Rebesco et al., 2013). A close interplay between downslope turbidity currents and alongslope contour currents is therefore expected when both processes occur on continental margins (Rebesco et al., 2002; Caburlotto et al., 2006; Brackenridge et al., 2013; Martorelli et al., 2016).

The continental margin offshore the Pearl River Mouth Basin (PRMB) is incised by deep-water submarine canyons and channels (Zhu et al., 2010). The most striking feature in the PRMB is the Baiyun Slide Complex, which has a large spatial coverage (~10,000 km^2) and is composed of several intersecting slide scars and overlapping deposits

* Corresponding author. CAS Key Laboratory of Ocean and Marginal Sea Geology, South China Sea Institute of Oceanology, Chinese Academy of Sciences, Guangzhou, 510301, PR China.
** Corresponding author. CAS Key Laboratory of Ocean and Marginal Sea Geology, South China Sea Institute of Oceanology, Chinese Academy of Sciences, Guangzhou, 510301, PR China.
E-mail addresses: wli@scsio.ac.cn (W. Li), sunjie@scsio.ac.cn (J. Sun).

https://doi.org/10.1016/j.marpetgeo.2020.104231
Received 25 March 2019; Received in revised form 11 December 2019; Accepted 8 January 2020
Available online 09 January 2020
0264-8172/ © 2020 Elsevier Ltd. All rights reserved.

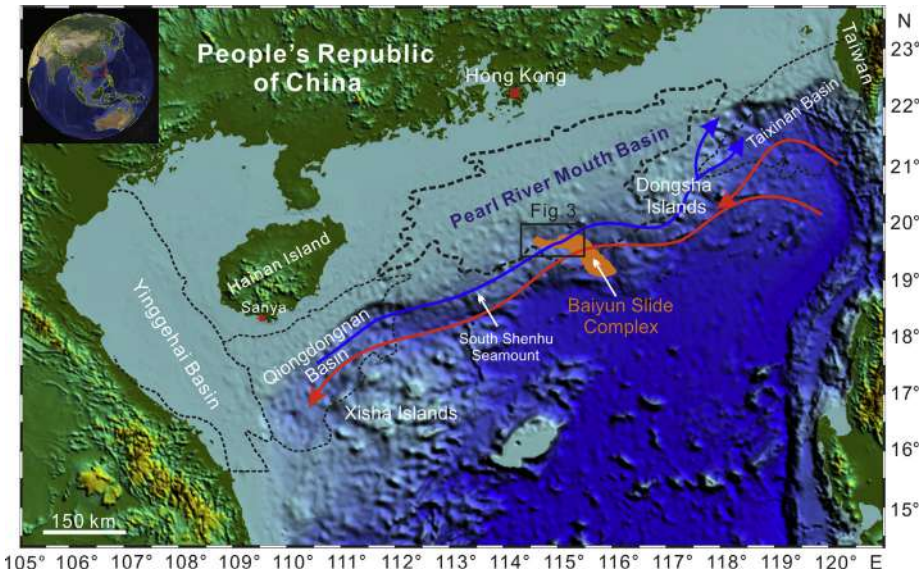

Fig. 1. Seafloor physiography of the northern South China Sea margin highlighting the distribution of the major sedimentary basins and bathymetric features such as the Dongsha Islands, the Xisha Islands and the South Shenhu Seamount. The blue and red curves indicate the paths of intermediate and deep waters offshore the northern South China Sea (Tian et al., 2006; Chen et al., 2014). The location of the Baiyun Slide Complex is marked in orange (Li et al., 2014). The black box indicates the location of the study area (see Fig. 2). (For interpretation of the references to colour in this figure legend, the reader is referred to the Web version of this article.)

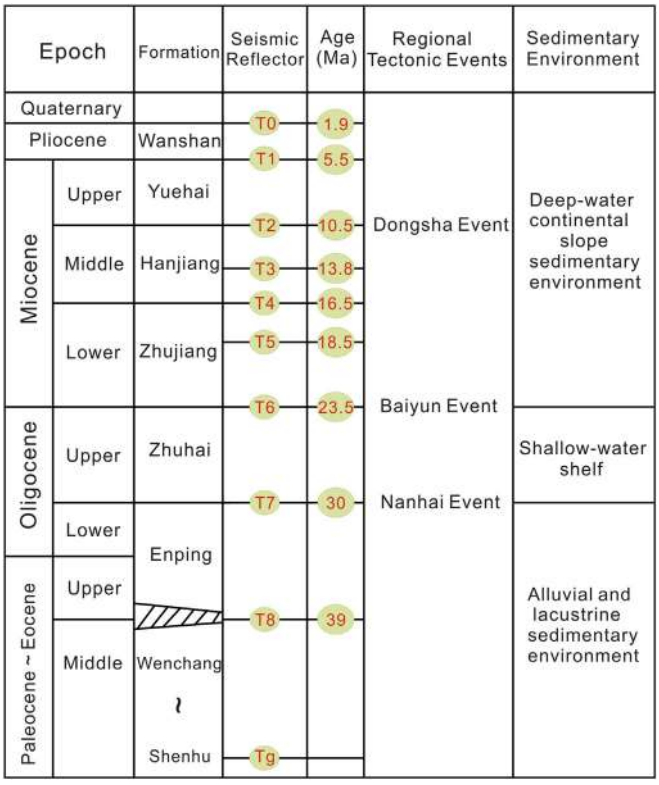

Fig. 2. (a) Multibeam bathymetry map of the study area illustrating the seafloor morphology of the headwall region of Baiyun Slide Complex, and the multiple submarine canyons observed here. The white lines reveal the location of seismic lines interpreted in this paper. The red box indicates the location of the headwall region of the Baiyun Slide Complex, which is shown in Fig. 5a. The location of Fig. 6b is marked by the purple box. (b) Contour map of the study area. The contour interval is 100 m. The red dashed line indicates the boundary of the Baiyun Slide Complex. Please see the location of Fig. 2 in Fig. 1. (For interpretation of the references to colour in this figure legend, the reader is referred to the Web version of this article.)

(Li et al., 2014; Sun et al., 2018b) (Fig. 1). The total volume of sediment removed by the Baiyun Slide Complex is ~1035 km^3 and comprises four major mass-transport deposits (MTDs) separated by basal erosional surfaces (Sun et al., 2018b). These MTDs retrograded upslope to reveal a decreasing time interval between events (Wang et al., 2017; Sun et al., 2018b). Two main instability events occurred in the headwall region of the Baiyun Slide Complex during the Quaternary (Li et al., 2014; Wang et al., 2017; Sun et al., 2018b), at ~0.79 Ma and ~0.54 Ma (Sun et al., 2018b). The older MTD (1570 km^2) covers most of the headwall region, while the younger MTD is mainly limited to the northern area of the headwall region to reveal a relatively smaller area of ~840 km^2 (Wang et al., 2017).

The study area is chiefly located in the headwall region of the Baiyun Slide Complex, at a water depth of 900 m–1800 m (Fig. 2a and b). This region is affected by alongslope bottom currents associated with a clockwise flow of intermediate water at a depth of 350 m–1350 m, and an anticlockwise flow of deep water at depths beyond 1350 m (Gong et al., 2013a,b; Chen et al., 2014) (Fig. 1). It provides a key opportunity to characterise how bottom currents, turbidity currents and submarine landslides influence the morphological and sedimentary evolution of the northern South China Sea margin. Hence, this work uses high-resolution bathymetric, 2D/3D seismic and borehole data are used to provide a detailed analysis of erosional and depositional features in and around the headwall region of Baiyun Slide Complex. The specific aims of this research are to:

a) investigate the seafloor morphology in and around the headwall region of the Baiyun Slide;
b) describe the internal seismic characters of the Baiyun Slide, and determine what are the main sedimentary processes in this area;
c) discuss the role of the Baiyun Slide Complex on the incision and development of submarine channels.

2. Geological and oceanographic background

2.1. Geological setting

The South China Sea is one of the largest (and deepest) marginal seas in the western Pacific Ocean (Fig. 1). The South China Sea as observed at present results from the formation of a proto-South China Sea, likely floored by oceanic crust, that was subducted during the Mesozoic (Pubellier et al., 2003). The earliest phase of rifting in South China Sea started in the latest Cretaceous to Early Paleocene and, after ~30 Ma of rifting, continental breakup was initiated first in its Eastern Sub-basin before ~32 Ma (Early Oligocene) (Barckhausen et al., 2014; Briais et al., 1993). Continued continental rifting led to the inception of continental breakup in the Southwest Sub-basin during the Late Oligocene, at ~25 Ma. In parallel to continental breakup, seafloor

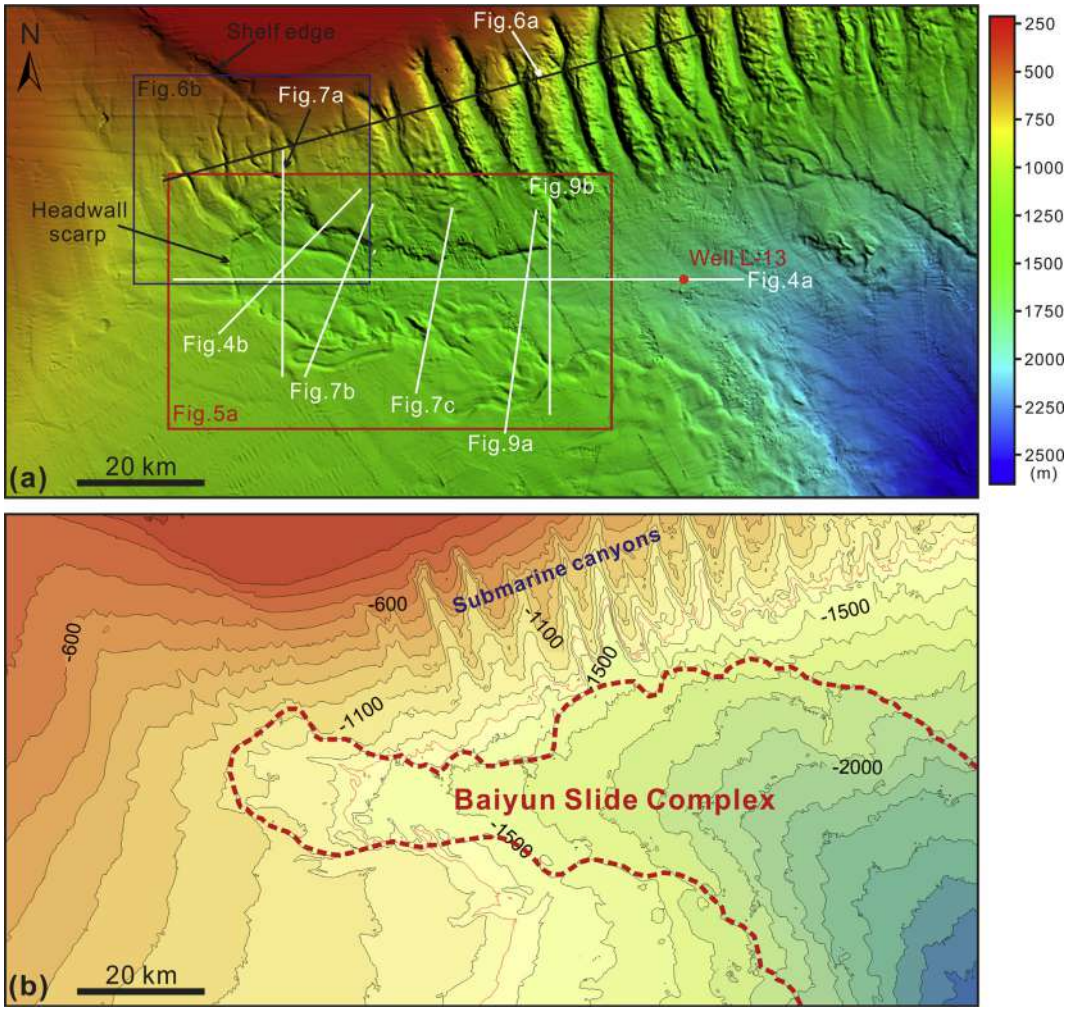

Fig. 3. Main stratigraphic units in the Pearl River Mouth Basin, regional tectonic events and resulting sedimentary environments (modified after Zhao et al., 2015).

spreading in the South China Sea followed the inception of continental breakup in distinct segments of the margin (Li et al., 2015a). Seafloor spreading in the South China Sea thus spans from 33 Ma to 15 Ma in the Northeast Sub-basin, and 23.6 Ma to 16 Ma in the Southwest Sub-basin based on the new results at IODP Site U1435 (Li et al., 2015a; Zhao et al., 2016).

The northern South China Sea margin has been influenced by seasonal alternations of the East Asian summer monsoon and the East Asian winter monsoon sub-regimes since, at least, the Late Miocene (Steinke et al., 2010). In the study area, the rate and composition of terrigenous sediment supplied to continental shelves, continental slopes and deep-sea basins has been largely influenced by changing monsoon conditions (Steinke et al., 2003, 2006). Intensified winter monsoon winds can increase wave heights in coastal zones, further amplifying sediment reworking processes. In such a setting, fine-grained fluvial sediment can be suspended in the water column to bypass the outer shelf and settle on the continental slope (Steinke et al., 2003, 2010).

The PRMB lies in the central part of the northern South China Sea and it is one of the most important hydrocarbon-rich basins in the region (Fig. 1). The geological evolution of the PRMB comprises three main stages: (1) a first rifting stage in the Late Cretaceous-Early Oligocene, essentially marked by continental rifting; (2) a transitional stage (Late Oligocene-Early Miocene) recording syn-breakup faulting, subsidence and deposition within distinct sub-basins; (3) a post-rift stage from the Middle Miocene to Holocene dominated by widespread subsidence and blanketing of syn-rift basins (Gong et al., 1989). In the PRMB regional tectonic uplift, faulting, erosion and magmatism are recorded in association with major tectonic events (Wu et al., 2014; Zhao et al., 2016). The most prominent tectonic event in the study area, the Dongsha Event, started in the Late Miocene (T2: 10.5 Ma; Fig. 3) and ceased around the Miocene/Pliocene boundary, at around 5.5 Ma (T1; Fig. 3; Wu et al., 2014). As a result of the Dongsha Event, a deep-water depositional setting was gradually developed after the Early Miocene, originating multiple submarine canyons, submarine channels on the continental slope and associated deep-water sediment fans (Fig. 3; Xie et al., 2006).

2.2. Oceanographic setting

Water masses in the South China Sea include a seasonally-influenced surface water and permanent intermediate- and deep-water masses (Tian et al., 2006; Chen et al., 2014) (Fig. 1). Surface water is controlled by the East Asia monsoon system and occurs at a water depth shallower than 350 m (Lüdmann et al., 2005; Contreras-Rosales et al., 2019). Surface water is clockwise during the summer and counter-clockwise during the winter (Zhu et al., 2010). Intermediate water (350 m–1350 m) follows a permanent clockwise movement and corresponds to the western boundary current in the South China Sea (Tian et al., 2006). It was established in the Late Miocene, resulting in: 1) the development of unidirectionally migrating deep-water channels in the Pearl River Mouth Basin (Zhu et al., 2010; Gong et al., 2013a,b), 2) the subsequent formation of depositional and erosional patterns around the South Shenhu Seamount (Chen et al., 2014) (Fig. 1). Deep water originates from the incursion of the southward flowing North Pacific Deep

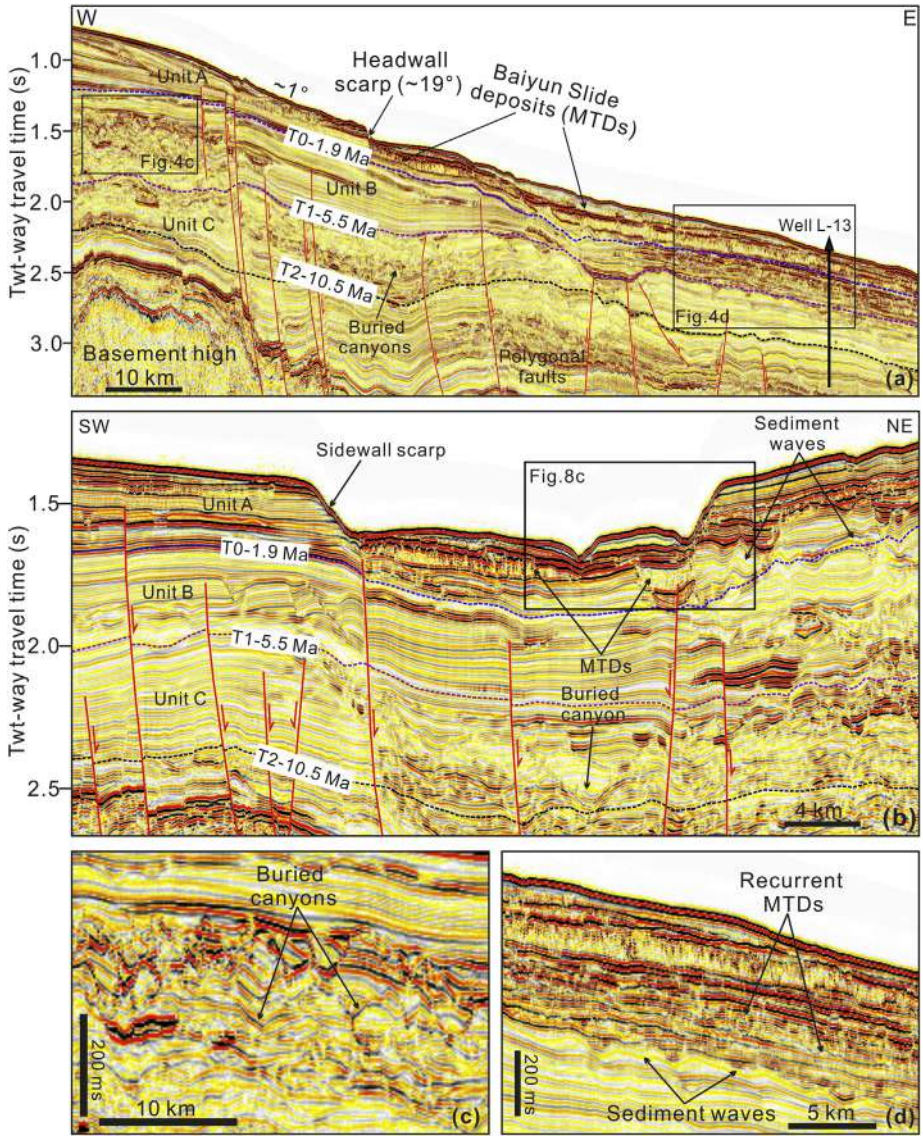

Fig. 4. (a) Three-dimensional seismic profile crossing the headwall region of Baiyun Slide Complex showing details of the headwall scarp and corresponding mass-transport deposits (MTDs) on the lower continental slope. (b) Zoomed in seismic profile (see location in Fig. 6a) revealing the presence of sediment waves beneath MTDs. (c) Zoomed in seismic profile on the lower continental slope below the headwall region. The profile illustrates the presence of recurrent MTDs. Please see the location of Fig. 4 in Fig. 2.

Water into the South China Sea via the Luzon Strait (Lüdmann et al., 2005). Widespread and thick sediment drifts occur to the southeast of the Dongsha Islands in association with deep-water currents, in places recording a maximum velocity of ~30 cm/s (Zhao et al., 2014).

3. Data and methods

High-resolution multibeam bathymetric data, 2D seismic profiles and 3D seismic volumes are used in this work. The bathymetric data was acquired at water depths ranging from 230 m to 2600 m and was positioned by a differential GPS. It was processed using the software CARIS HIPS®. Its horizontal and vertical resolutions are ~100 m and ~1–3.3 m, respectively, enabling the identification and analysis of seafloor features generated by downslope and alongslope currents.

The interpreted seismic dataset was acquired and processed by China National Offshore Oil Corporation (CNOOC) and covers the headwall region of the Baiyun Slide Complex. It consists of one long (~100 km) 2D seismic profile crossing submarine canyons and channels on the continental slope, and ~4000 km^2 of 3D seismic data. The dominant frequency of the 2D seismic data is ~30 Hz, and its vertical resolution ranges from 15 to 20 m. The 3D seismic data has a dominant frequency of 40–60 Hz in the interval of interest, providing a vertical resolution of about 10–15 m. This relatively high resolution of the seismic data enabled the detailed investigation of sedimentary features in the headwall region of Baiyun Slide Complex (Fig. 4a).

Exploration Well L-13 was drilled in the central part of the study area and provided age constrains for the interpreted seismic horizons (Fig. 2a). Main seismic reflections were identified and traced using Schlumberger's Geoframe® 4.5 so that a regional seismic-stratigraphic framework could be built for the study area. Three important seismic horizons (T0, T1 and T2) were recognised and dated as 1.9 Ma, 5.5 Ma and 10.5 Ma in age (Fig. 4a).

4. Seismic stratigraphy

The seismic stratigraphy of the study area was interpreted and tied to borehole data from Exploration Well L-13. Three main seismic units, named as Units A, B and C from top to bottom, were identified based on

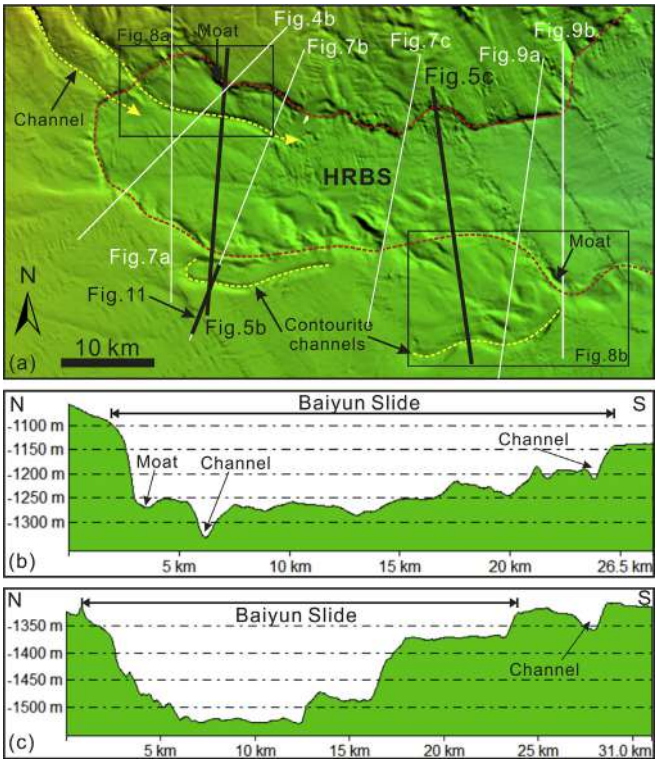

Fig. 5. (a) Multibeam bathymetric map showing the detailed seafloor morphology of the headwall region of the Baiyun Slide Complex. The escarpment in the headwall region of the Baiyun Slide is marked by a red dashed line. The yellow dashed lines indicate the location of submarine channels on the modern sea floor. The black solid lines represent the bathymetric profiles in Fig. 5b and c. Please see the location of Fig. 5a in Fig. 2a. (b) Bathymetric profile crossing the headwall region of the Baiyun Slide and revealing the presence of submarine channels. (c) Bathymetric profile revealing the presence of submarine channels in the headwall region. HRBS: headwall region of the Baiyun Slide. (For interpretation of the references to colour in this figure legend, the reader is referred to the Web version of this article.)

the differences in their internal reflection configurations (Fig. 4a and b).

Unit A is bounded by T0 at its base and its top coincides with the sea floor (Fig. 4a). Unit A is suggested to be Quaternary in age. On the upper continental slope, moderate-to high-amplitude reflections predominate (Fig. 4a). Downslope, widespread chaotic seismic reflections suggest the presence of MTDs (Fig. 4d). The most prominent feature in Unit A is the slide scar from the Baiyun Slide Complex, herein named Baiyun Slide scar, and MTDs resulting this latter instability feature (Fig. 4b).

Unit B is Pliocene in age and bounded by seismic horizons T1 and T0 (Fig. 4a and b). Seismic facies in Unit B change in different parts of the study area (Fig. 4a). In the upper slope region, several submarine canyons can be identified (Fig. 4a and c). In the middle sector of the slope, Unit B shows continuous moderate-amplitude reflections (Fig. 4a). Strata downslope from this latter region shows chaotic seismic reflections bounded by irregular top and bottom surfaces (Fig. 4a and d), likely comprising MTDs. Unit B shows variable thickness in the E-W seismic profile in Fig. 4a.

Unit C is bounded by seismic horizon T2 at its bottom and T1 at its top. Unit C is Late Miocene in age and shows low-to moderate-amplitude reflections (Fig. 4a and b). A main valley and several buried submarine canyons are observed in the middle part of Unit C (Fig. 4a). The thickness of Unit C is variable on the E-W seismic profile in Fig. 4a, but shows a constant thickness on the SW-NE oriented seismic profile in Fig. 4b. Several large-scale faults can be observed cutting through Unit C.

5. Seafloor morphology

Seafloor morphology is uneven in the study area (Figs. 2a and 5a). Different kinds of morphological features can be identified, with the most prominent feature being the Baiyun Slide scar (Fig. 2a).

5.1. Baiyun Slide scar

The headwall region of the Baiyun Slide Complex displays a U-shaped slide scar that opens towards the east with a length of ~50 km and an average width of 14 km (Figs. 2a and 5a). This scar is located at a water depth between 1100 m and 1600 m and covers an area of ~700 km^2 (Fig. 2a and b). The northern escarpment of the scar is ~45 km-long and consists of several smaller-scale scars (Fig. 5a). In the south, the escarpment shows a length of ~50 km and appears to be disrupted by several ridges. The headwall scarp has an average height of ~90 m and a slope gradient of up to 19° (Figs. 2a and 4a). The escarpment of the slide scar is much steeper in the north (up to 22°) than in the south (~5°), as shown on the bathymetric profiles crossing the slide scar (Fig. 5b and c). The undeformed seafloor has a gradient of ~1° (Fig. 4a).

5.2. Submarine canyons and channels

Submarine canyons are usually not connected to a modern river, and have near-vertical walls that extend well onto the continental shelf. Submarine channels are smaller, usually meandering, and comprise a thalweg and confining levees (Shepard, 1936, 1981; Amblas et al., 2018). They are less steep than canyons and are commonly within canyons themselves - it is not uncommon to record channel systems at the bottom of canyons. To the north of the headwall area of the Baiyun Slide Complex occur seventeen (17) submarine canyons, as already documented by Zhu et al. (2010), Gong et al., 2013a,b and Ma et al. (2015). In this study, only seven of these canyons are fully imaged on the newly–acquired bathymetric data, towards the western part of the complex (Fig. 2a). The orientation of these submarine canyons is NNW-SSE, and is perpendicular to the continental slope. These submarine canyons are sub-linear and sub-parallel in plan view, displaying a regular spacing of 8–10 km. They are located at water depths ranging from 500 m to 1500 m (Fig. 2b). As observed on the contour map in Fig. 2b, these submarine canyons are confined on the continental slope and do not erode the shelf edge, which occurs at a water depth of ~200 m. These submarine canyons are about 20–40 km-long, 3-5 km-wide and incise the slope to a depth of 100–300 m. The bathymetric profile crossing the submarine canyons shows that canyon flanks are steep and display V-shaped geometries (Fig. 6a). Compared to the large-scale submarine canyons, several small-scale submarine channels (A1 to A6) can be clearly distinguished on the upper continental slope above the headwall region (Figs. 2a, 6b and 6c; Table 1). These submarine channels are 16–37 km-long, 800-1500 m-wide and 20 to 50 m-deep (Fig. 6b). Some of these channels (A2-A3 and A4-A5) incise the headwall scarp to extend into the upper part of the Baiyun Slide Complex (Figs. 2a and 5a).

6. Morphology and internal character of the Baiyun Slide scar

6.1. Slide scarps and mass-transport deposits (MTDs)

The headwall and sidewall scarps of the Baiyun Slide Complex can be readily identified on the bathymetric map and seismic profiles (Figs. 2a, 4a and 7a). The slide scarps are steep and adjacent intact strata show obvious erosional truncations (Figs. 4b and 7b). Most MTDs are located in Units A and B, especially downslope from the slide headwall where recurrent MTDs are observed (Fig. 4a and c). The uppermost MTD shows a thickness of ~75 m (Fig. 4c and d). Beneath this MTD, several smaller-scale MTDs are vertically stacked and naturally

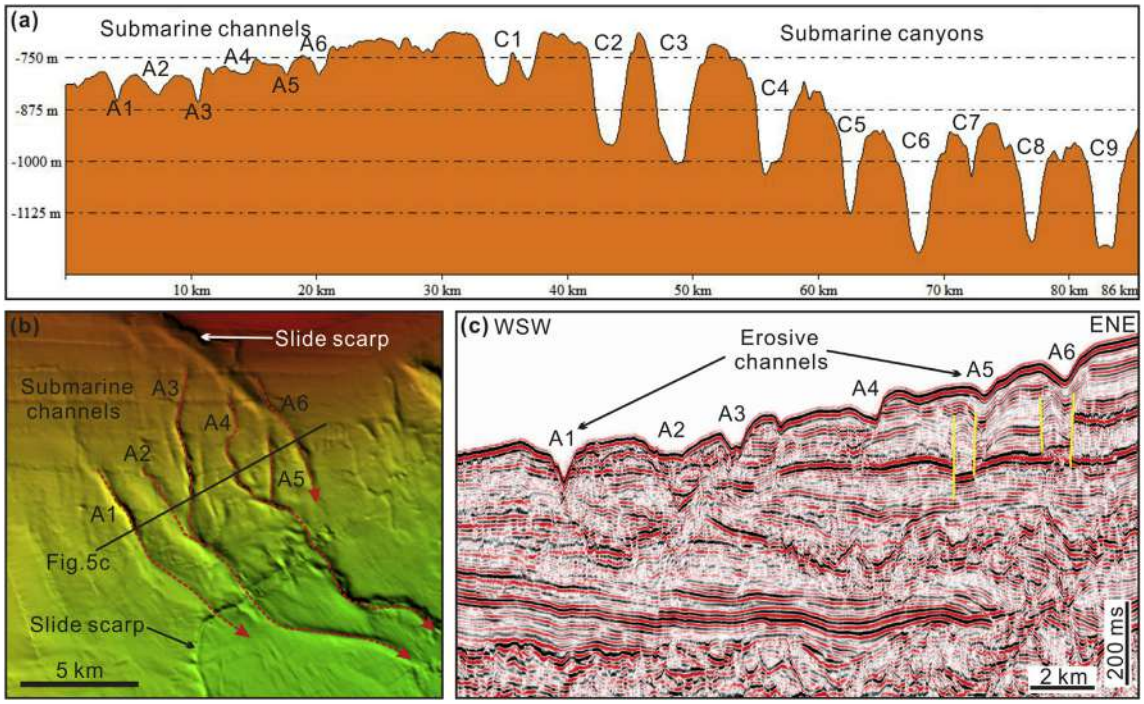

Fig. 6. (a) Bathymetric profile crossing submarine canyons C1 to C9 and submarine channels A1 to A6 in the upper continental slope region of the Baiyun Slide Complex (see location in Fig. 3). Note that submarine canyons (C1 to C9) show a much larger incision depth than submarine channels A1 to A6. Please see the location of Fig. 6a in Fig. 3a. (b) Multibeam bathymetric map showing the detailed seafloor morphology of submarine channels A1 to A6. (c) Two-dimensional seismic profile revealing the internal architecture of submarine channels above the headwall region of the Baiyun Slide Complex. See location of the seismic profile in Fig. 6b.

Table 1
Morphological parameters, including widths, lengths, incised depths, and dip angles of the southwestern (SW) and northeastern (NE) flanks of the submarine channels identified around the Baiyun Slide scar.

Channels	A1	A2	A3	A4	A5	A6
Width (m)	~900	~1500	~800	~1000	~900	~1400
Length (km)	~24	~33	~37	~32	~26	~16
Incised Depth (m)	~73	~22	~52	~34	~42	41
SW Flank (°)	~10	~3	~7	~4	~7	~3
NE Flank (°)	~11	~5	~16	~7	~8	~4

increase the total thickness of mass-wasting deposits on the continental slope (Fig. 4c). Compared to the seismic profiles imaging the lower continental slope, relatively thin MTDs can be identified within the headwall area of the Baiyun Slide Complex (Fig. 7a and c).

6.2. Erosive channels and moats

Six submarine channels are observed on the bathymetric map and on seismic data (Figs. 4b, 6b and 7 and 8). A submarine channel generated by the confluence of channels A2 and A3 incises the seafloor in the uppermost (westward) part of the Baiyun Slide Complex (Fig. 5a and b). This channel has a width of approximately 2 km and a depth of about 50 m (Figs. 5b and 8a). It cuts the headwall scarp of the Baiyun Slide Complex and extends farther towards the east. Seismic reflections crossing the submarine channel are not continuous, and erosional truncations can be observed on both flanks of the channel (Fig. 8c and d). Two other erosive channels are located in the southern part of its headwall region (Fig. 5a). They have an E-W orientation, parallel to the southern escarpment of the slide scar.

Elongated depressions can be observed on the bathymetric map and seismic profiles located in the vicinity of the slide scarps (Fig. 8a, b and c). Strata close to these depressions typically show mounded shapes (Fig. 8c). Such features can be interpreted as moats, i.e. localised erosional features with little effect other than forming channeled paths for sediment that is redistributed along the slope (Rebesco et al., 2007; García et al., 2009). Mounded strata comprise sediment drifts (Figs. 7b and 8c), as their most distinctive feature is the termination of internal reflections towards the moat (Rebesco et al., 2016).

6.3. Sediment waves

Sediment waves are observed at different locations within and around the Baiyun Slide Complex, such as those within the slide scar (Fig. 7c) and south of the slide scar (Fig. 9a and b and 10b). Internal seismic reflections within the sediment waves are continuous, showing moderate to low amplitude (Fig. 10a and b). Continuous internal reflections can be traced across adjacent waves. Sediment waves show a variety of dimensions, with their length ranging from 2 km to 4 km and height varying from 30 m to 70 m. The crests of sediment waves within the slide scar typically show upslope migration trends and an asymmetric geometry (Fig. 10a). The sediment waves in the southern part of the slide scar are dominated by vertical aggradation, rather than upslope migration (Fig. 10b). Deposition occurs both on their upslope and downslope flanks, forming symmetrical sediment waves.

6.4. Migrating channels

Buried channels are widely observed and some show typical unidirectional migration (Figs. 7b and 11). Buried migrating channels are located in the southern part of the headwall region. The base of these channels coincides with an unconformity which, on seismic data, is shown as a continuous and high-amplitude concave reflection (Fig. 11). The thalweg of a buried channel in the shallower area (water depth < 1500 m) is progressively offset towards the north and the unidirectional migration distance of its thalweg reaches 3 km (Fig. 11). In parallel, MTDs are observed within the channel and are likely the

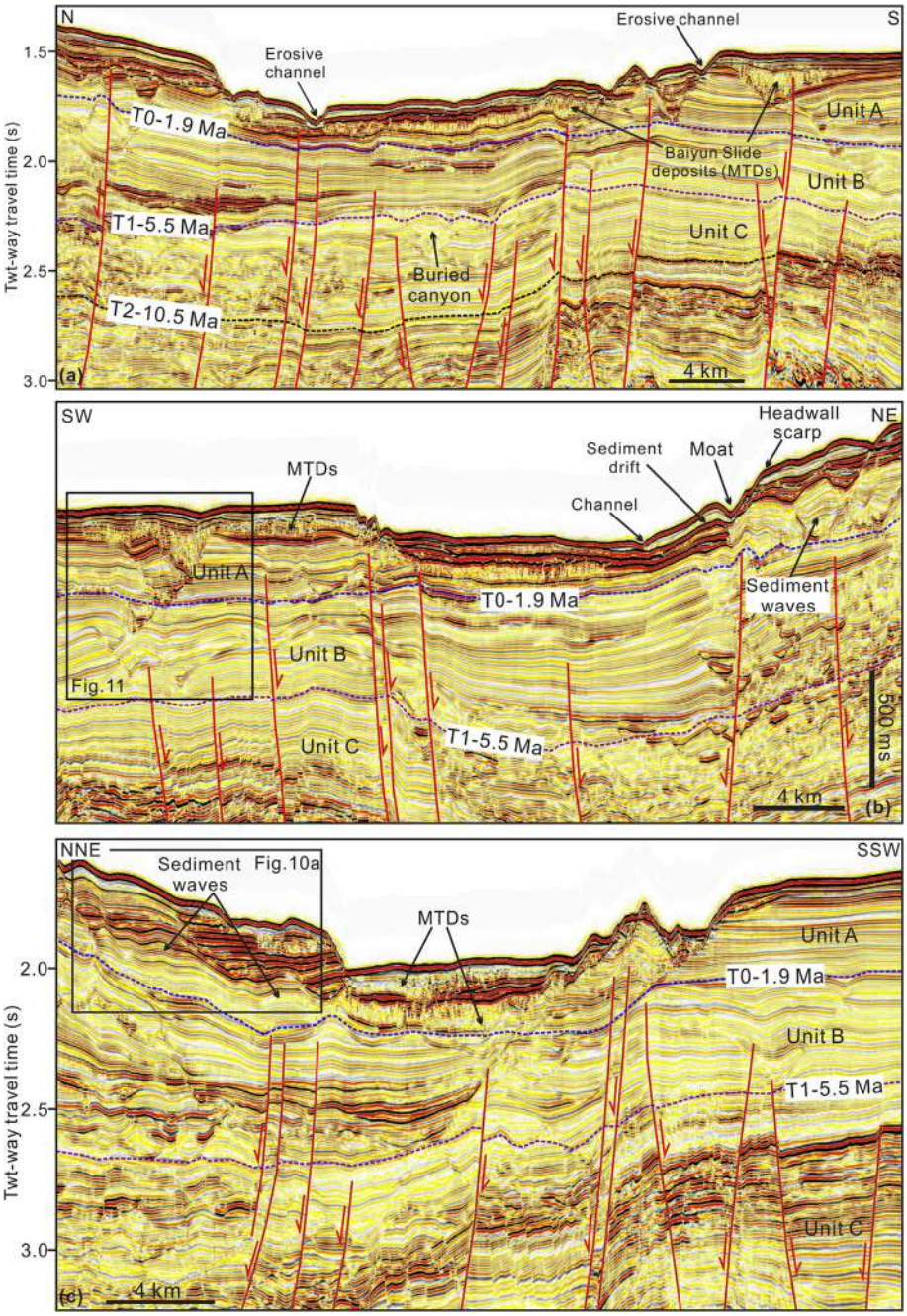

Fig. 7. Three high-resolution seismic profiles crossing different locations of the headwall region to reveal its detailed internal architecture. (a) 3D seismic profile revealing the presence of buried submarine canyons, MTDs, large-scale faults and erosive channels on the modern sea floor. (b) A moat and buried sediment waves can be identified in the northern part of the headwall region. A migrating channel is located in the southern part of the headwall region, as shown in detail in Fig. 11a. (c) 3D seismic profile imaging sediment waves in the northern part of the headwall region, as shown in detail in Fig. 10a. Location of Fig. 7 in Figs. 2a and 5a.

main depositional elements of the channel fills (Fig. 11).

7. Discussion

7.1. Importance of combined downslope and alongslope processes on a sediment-fed continental slope

We propose that the headwall region of the Baiyun Slide Complex was affected by both downslope and alongslope sedimentary processes since its inception as: (a) it is located at a water depth influenced by intermediate (350 m–1350 m) and deep-water currents (> 1350 m); and (b) it is close to submarine canyons incising the continental slope in the same place where submarine slides and turbidity currents occurred frequently in the past. In this work, several types of depositional and erosional features are identified, demonstrating the influence of turbidity currents, contour currents and sediment mass-wasting on the geomorphology of the headwall of the Baiyun Slide Complex, and around it.

MTDs are mainly identified in Unit A and B, indicating that downslope sedimentary processes have been active since the latest Miocene. The uppermost two MTDs have been interpreted as the slide deposits marking the last stages of slope instability in the Baiyun Slide Complex (Li et al., 2014; Wang et al., 2017; Sun et al., 2018b), and were respectively dated as 0.54 Ma and 0.79 Ma based on seismic-stratigraphy correlations with ODP Site 1146 (Sun et al., 2017). Other MTDs are noticeably smaller and might have been sourced from adjacent

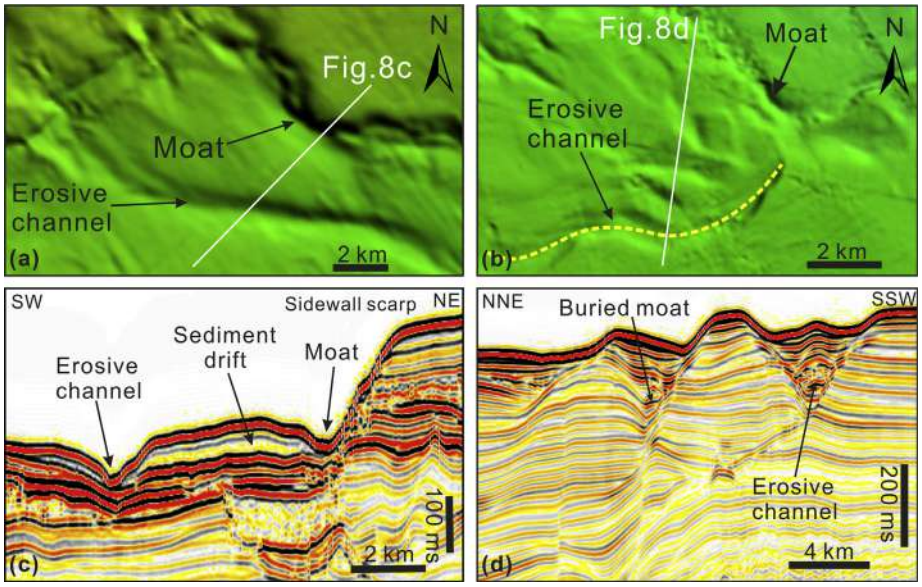

Fig. 8. Enlarged seismic sections (a–d) illustrating the moat and sediment drift developed close to the southern sidewall scarp of the Baiyun Slide Complex. Erosive channels and related truncations can be observed on the modern sea floor.

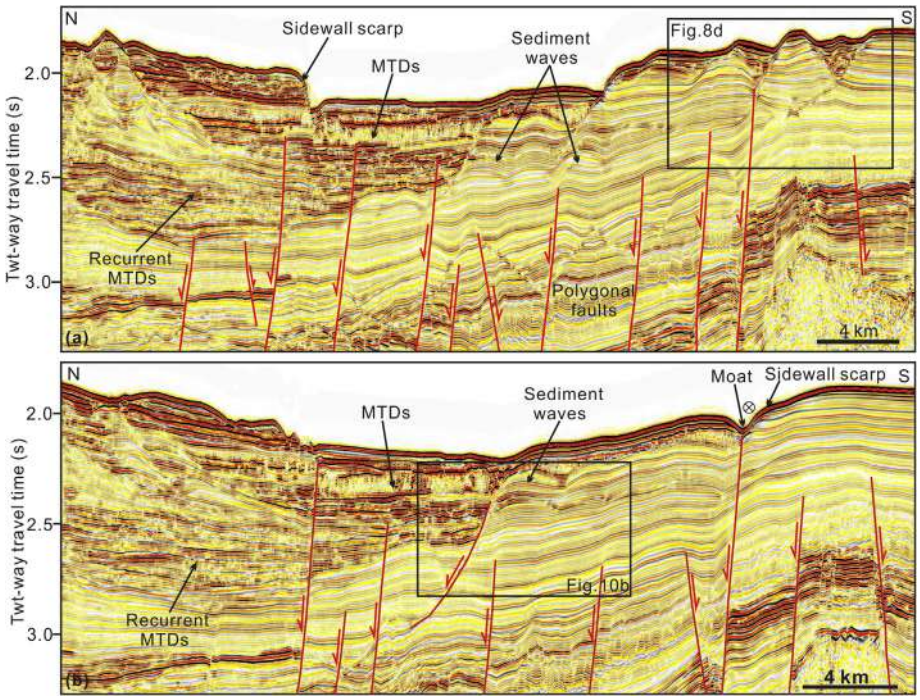

Fig. 9. (a) 3D seismic profile crossing the eastern part of the headwall region to show sediment waves buried by recurrent MTDs. A buried moat and a submarine channel can be observed in the southern part of the headwall region. (b) 3D seismic profile illustrating a moat close to the sidewall scarp of the Baiyun Slide. A large-scale fault has propagated very close to the sea floor. Location of Fig. 9 in Figs. 2a and 5a.

submarine canyons. Multiple scars of submarine landslides associated with submarine canyons have been mapped in this region based on their characteristic headscarps and basal shear surfaces (He et al., 2014; Chen et al., 2016). These submarine landslides are mostly distributed around the canyon heads and flanks, and some were able to further disintegrate and evolve into turbidity currents flowing along the submarine canyons (Chen et al., 2016).

Buried sediment waves observed in the large slide scar identified in this work are asymmetric with gentle upslope flanks and steep downslope flanks (Figs. 6c and 9a). These sediment waves have thicker beds on their stoss side and their crests exhibit an upslope migration trend (Fig. 10a). Internal seismic reflections within these sediment waves are continuous and can be traced from one wave to the next. In addition, they are very close to submarine canyons incising the upper continental slope, where turbidity currents occur more frequently. Based on the criteria of Wynn and Stow (2002), these sediment waves can be interpreted as formed by turbidity currents flowing through submarine canyons on the upper continental slope. Once the initial sediment wave topography is established, the process leading to wave migration and growth was self-perpetuating (Normark et al., 2002). Sediment waves with similar internal seismic characters have also been documented in the Magdalena turbidite system (Ercilla et al., 2002), on the South Iberian Margin (Perez-Hernandez et al., 2014) and on the South China Sea slope offshore SW Taiwan (Gong et al., 2012, 2015), where the genesis of sediment waves is considered to result from turbidity currents. Additionally, erosive channels on the upper continental slope may also be formed by the erosion of turbidity currents, which were probably initiated by the transformation of slumps or storm-generated

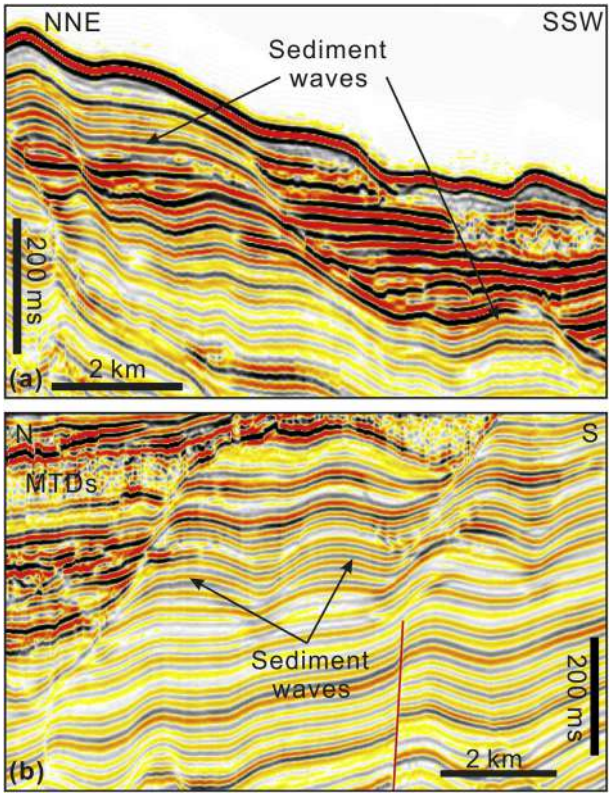

Fig. 10. (a) Zoomed-in seismic profile showing the internal architecture of sediment waves in the northern part of the headwall region, close to the submarine canyons crossing the upper continental slope. See location of the profile in Fig. 7. (b) Zoomed in seismic profile revealing the presence of sediment waves in the southern part of the headwall region. See location of the seismic profile in Fig. 9b.

flows near the shelf edge (Figs. 2a and 7d).

Two moats and associated sediment drifts have been identified close to slide scarps formed at the headwall of the Baiyun Slide (Figs. 4a and 7c), indicating enhanced activity of bottom currents after the formation of the observed slide scar - uneven seafloor bathymetry may locally intensify and focus bottom-current activity (García et al., 2009; Vandorpe et al., 2016; Martorelli et al., 2016). The moats can be used to reconstruct the path of the inferred bottom current flow that controlled the development of sediment drifts (Surlyk and Lykke-Andersen, 2007; Rebesco et al., 2016). The two erosive channels in the southern part of the slide scar are interpreted as contourite channels as they are far away from the influence of turbidity currents (Figs. 2a, 6b and 8a and b). In comparison, the sediment waves also observed in the southern part of the slide scar are relatively more symmetric with continuous, parallel to sub-parallel internal reflections, suggesting sediment aggradation rather than upslope migration (Fig. 8a and b). This internal character is consistent with that observed from bottom-current sediment waves (Gong et al., 2015; Baldwin et al., 2017).

Of particularly interest is the identification on bathymetric data of an erosive channel to the south of the Baiyun Slide scar (Fig. 5a). This channel has no obvious levee and its base migrates progressively northwards (Figs. 7b and 11). We interpret this channel as an unidirectionally migrating channel similar to those documented on the northern South China Sea margin (He et al., 2013; Gong et al., 2013a,b, 2018), on the continental rise of southeast Greenland (Rasmussen et al., 2003) and along the continental margin of Equatorial Guinea (Jobe et al., 2011). The presence of this unidirectionally migrating channel suggests a close interaction between episodic downslope gravity (or turbidity) flows and persistent alongslope bottom (contour) currents.

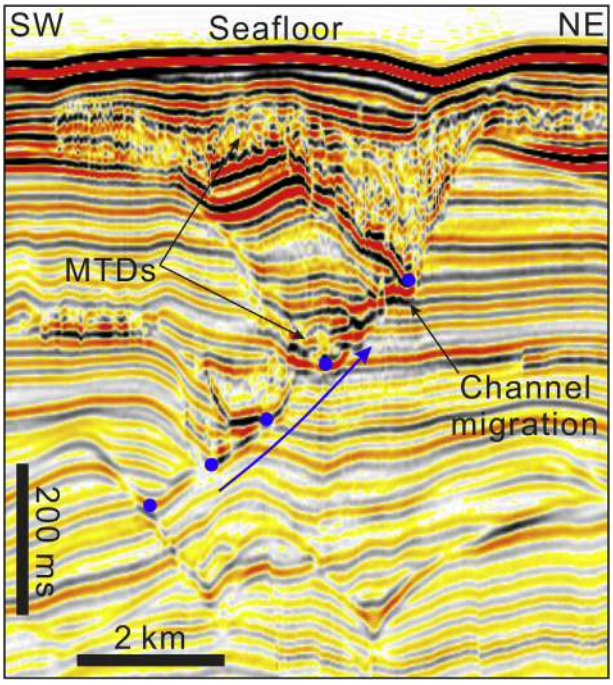

Fig. 11. Interpreted seismic profile from the southern part of the headwall region revealing a buried submarine channel. The blue dots represent the base of the buried channel, which reveal a N–S migration trend at start to then migrate towards the north. Please see the location of Fig. 11 in Fig. 5a. (For interpretation of the references to colour in this figure legend, the reader is referred to the Web version of this article.)

7.2. The role of slide scars on the initiation and formation of submarine channels

The bathymetric map covering the headwall of the Baiyun Slide Complex reveals the presence of several submarine channels (Figs. 4a and 5b). These submarine channels with a general NW-SE orientation incise the headwall scarp of the Baiyun Slide Complex and erode the Baiyun Slide scar farther – up to a maximum distance of 10 km from the headwall (Figs. 2a, 5a and 6b). The submarine channels are close to submarine canyons and have similar orientations (Fig. 2a).

The bathymetric profile crossing the submarine canyons and channels reveals conspicuous differences in their scales and incision depths (Fig. 6a). Submarine canyons have been present in the study area, since the Middle Miocene, at least (Gong et al., 2013a,b; Ma et al., 2015), but the timing of formation of channels has not been constrained in the literature. Truncations can be clearly observed on seismic profiles crossing the observed submarine channels (Figs. 4b, 7a and 8c), which eroded the draped strata above the MTDs up to a depth of ~60 m (Fig. 5b). These data provide a robust proof that these submarine channels were formed after the Baiyun Slide Complex was initiated (Fig. 4b). Therefore, we propose that submarine channels identified around the Baiyun Slide scar are relatively newly-formed erosional features compared to the longer-lived submarine canyons.

Based on the detailed interpretation of bathymetry and seismic data, we propose a conceptual model to explain the morphological evolution of the study area (Fig. 12). The Baiyun Slide Complex evacuated large volumes of sediment (~1035 km^3) and greatly changed the slope morphology (Fig. 12a and b; Li et al., 2014; Sun et al., 2018a). In addition, the formation of the Baiyun Slide scar was able to enhance local accommodation space for subsequent turbidity currents and mass-wasting deposits (Fig. 12b and c). We therefore suggest that the formation of the Baiyun Slide scar played a vital role on the initiation and formation of the submarine channels identified on the upper part of the continental slope. Qin et al. (2017) also found that slide scars can

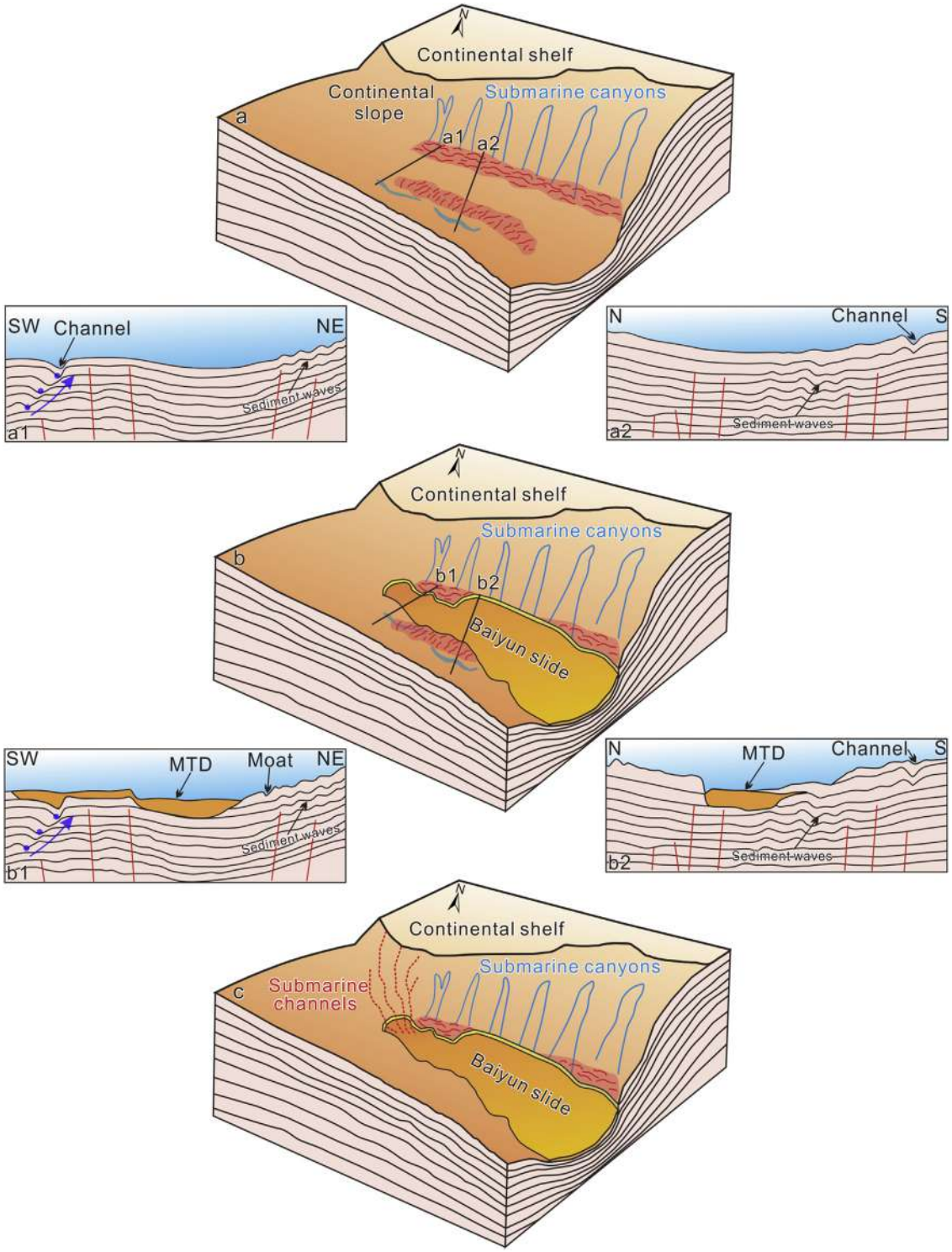

Fig. 12. Conceptual model summarizing the evolution of the Baiyun Slide scar. (a) The continental slope was incised by several submarine canyons. The sediment waves in the north were formed by turbidity currents flowing through the submarine canyons (a1), while those in the south resulted from the interaction of bottom currents with the seafloor (a2). A submarine channel reveals a migration pattern towards northeast (b) The Baiyun Slide occurred downslope from the submarine canyons and evacuated large volumes of sediment (~1035 km^3) on the sea floor. The Baiyun Slide eroded the sediment wave fields and resulting MTDs filled the laterally migrating channel in the south (b1 and b2). (c) Several submarine channels formed after the Baiyun Slide Complex erode its headwall scarps.

capture turbidity flows and facilitate flow channelisation, both key processes for the initiation of submarine channels in the Espírito Santo Basin, SE Brazil. In addition, Abdurrokhim and Ito (2013) have investigated the role of slump scars as initial seafloor features responsible for the formation of slope channels in the Bogor Trough, West Java. Initial depressions, and seafloor roughness induced by slump scars and by mass-transport deposits, may develop an area of sediment-gravity flow convergence that is later able to locally incise the continental slope to form submarine channels (Alves and Cartwright, 2010; Qin et al., 2017).

The submarine channels in the upper part of the Baiyun Slide scar are V-shaped in cross-section (Figs. 4b, 5a and 6b) and their upper

reaches are close to the shelf edge (Figs. 2a and 6a). Several other small-scale landslide scarps close to the shelf edge are imaged on high-resolution bathymetric data (Figs. 2a and 6b). They may result either from large, unconfined and erosive turbidity currents or from mass wasting. In such a setting, channels are suggested to be the first features to form on steeply dipping slopes sculpted by mass wasting (e.g. Lonergan et al., 2013; Laberg et al., 2007). Micallef and Mountjoy (2011) have also proposed gravity flows to be responsible for initiating V-shaped channels in the Cook Strait, New Zealand. The importance of interacting turbidity currents and seafloor roughness on channel initiation has also been stressed by Gee et al. (2007) and Covault et al. (2014). Hence, the incision of submarine channels in the study area can be considered as an indicator of intensified downslope sedimentary processes (e.g. turbidity currents and mass wasting) after the Baiyun Slide scar was formed. As for the triggering factors increasing downslope sedimentary gravity flows, Wang et al. (2018) proposed that the long-term erosion by contour currents associated with the South China Sea Branch of the Kuroshio Current caused the slope to become unstable and prone to collapse.

8. Conclusions

High-resolution bathymetry and 2D/3D seismic data enabled us to investigate the headwall region of Baiyun Slide Complex on the northern South China Sea in terms of its morphology, associated sedimentary processes and its role on the initiation of submarine channels. The main conclusions of this study are as follows:

(1) The headwall region of Baiyun Slide Complex has a U-shaped morphology in plan view at a water depth between 1000 m and 1700 m. Sediment was almost completely evacuated from the slide complex, leaving pronounced headwall and sidewall scarps.
(2) Sediment waves, moats, erosional channels and migrating channels were identified inside and around the headwall of the Biyun Slide Complex. Downslope and alongslope sedimentary processes have controlled and affected the overall bathymetry inside and around the latter headwall region.
(3) Sediment waves identified downslope from submarine canyons were generated by turbidity currents, while those observed in the southern part of the Baiyun Slide scar were generated by bottom currents interacting with the sea floor. The presence of migrating channels in the study area reveals a close interaction between downslope and alongslope sedimentary processes.
(4) The submarine channels in the upper part of the Baiyun Slide scar are Quaternary in age and were formed after this latter bathymetric feature. The submarine channels mark the intensification of downslope sedimentary processes (e.g. turbidity currents and mass wasting) over alongslope processes after the Baiyun Slide scar was formed.

This research is an important case study of the role of submarine landslides on regional sedimentary processes. Our results are also of importance to characterise the sedimentary processes operating on continental margins, where a close interplay between downslope and alongslope currents occurred in the past.

Author contribution section

Wei Li: Conceptualization, Writing- Original draft preparation, Funding acquisition. **Tiago M. Alves:** Conceptualization, Writing-Reviewing and Editing. **Michele Rebesco:** Writing- Reviewing and Editing.**Jie Sun:** Visualization. **Jian Li:** Visualization. **Shuang Li:** Visualization. **Shiguo Wu:** Writing- Reviewing and Editing.

Acknowledgments

We acknowledge China National Offshore Oil Corporation for their permission to release the seismic data. Dr. Neil C. Mitchell is thanked for his invaluable assistance and fruitful discussion, which improved this paper. This work was financially supported by the Innovation Development Fund of South China Sea Eco-Environmental Engineering Innovation Institute of the Chinese Academy of Sciences (ISEE2018PY02), National Scientific Foundation of China (41876054), National Key Research and Development Program of China (2017YFC1500401) and Key Laboratory of Ocean and Marginal Sea Geology, Chinese Academy of Sciences (OMG18-09). The bathymetric maps in this study were produced through Global Mapper 11 and Surfer 10. Dr. Wei Li is funded by CAS Pioneer Hundred Talents Program (Y8SL011001). The paper benefited from the constructive comments of the editor, Dr. Daniele Casalbore and two anonymous reviewers.

References

Abdurrokhim, Ito, M., 2013. The role of slump scars in slope channel initiation: a case study from the Miocene Jatiluhur Formation in the Bogor Trough, West Java. J. Asian Earth Sci. 73, 68–86.
Alves, T.M., Cartwright, J.A., 2010. The effect of mass-transport deposits on the younger slope morphology, offshore Brazil. Mar. Pet. Geol. 27, 2027–2036.
Amblas, D., Ceramicola, S., Gerber, T.P., Canals, M., Chiocci, F.L., Dowdeswell, J.A., Harris, P.T., Huvenne, V.A.I., Lai, S.Y.J., Lastras, G., Iacono, C.L., Micallef, A., Mountjoy, J.J., Paull, C.K., Puig, P., Sanchez-Vidal, A., 2018. Submarine canyons and gullies. In: Micallef, A., Krastel, S., Savini, A. (Eds.), Submarine Geomorphology. Springer International Publishing, Cham, pp. 251–272.
Baldwin, K.E., Mountain, G.S., Rosenthal, Y., 2017. Sediment waves in the Caroline Basin suggest evidence for Miocene shifts in bottom water flow in the western equatorial Pacific. Mar. Geol. 393, 194–202.
Barckhausen, U., Engels, M., Franke, D., Ladage, S., Pubellier, M., 2014. Evolution of the South China Sea: revised ages for breakup and seafloor spreading. Mar. Pet. Geol. 58, 599–611.
Bourget, J., Zaragosi, S., Ellouz-Zimmermann, N., Mouchot, N., Garlan, T., Schneider, J.-L., Lanfumey, V., Lallemant, S., 2011. Turbidite system architecture and sedimentary processes along topographically complex slopes: the Makran convergent margin. Sedimentology 58, 376–406.
Brackenridge, R.E., Hernández-Molina, F.J., Stow, D.A.V., Llave, E., 2013. A Pliocene mixed contourite–turbidite system offshore the Algarve Margin, Gulf of Cadiz: seismic response, margin evolution and reservoir implications. Mar. Pet. Geol. 46, 36–50.
Briais, A., Patriat, P., Tapponnier, P., 1993. Updated interpretation of magnetic anomalies and seafloor spreading stages in the South China Sea: implications for the Tertiary tectonics of Southeast Asia. J. Geophys. Res. 98, 6299–6328.
Caburlotto, A., De Santis, L., Zanolla, C., Camerlenghi, A., Dix, J.K., 2006. New insights into Quaternary glacial dynamic changes on the George V Land continental margin (East Antarctica). Quat. Sci. Rev. 25, 3029–3049.
Casalbore, D., Romagnoli, C., Chiocci, F., Frezza, V., 2010. Morpho-sedimentary characteristics of the volcaniclastic apron around Stromboli volcano (Italy). Mar. Geol. 269, 132–148.
Casalbore, D., Martorelli, E., Bosman, A., Morelli, E., Latino Chiocci, F., 2018. Failure dynamics of landslide scars on the lower continental slope of the Tyrrhenian Calabrian margin: insights from an integrated morpho-bathymetric and seismic analysis. Geological Society, London, Special Publications 477 SP477.416.
Chen, H., Xie, X., Rooij, D.V., Vandorpe, T., Su, M., Wang, D., 2014. Depositional characteristics and processes of along slope currents related to a seamount on the northwestern margin of the Northwest Sub-Basin, South China Sea. Mar. Geol. 355, 36–53.
Chen, D., Wang, X., Völker, D., Wu, S., Wang, L., Li, W., Li, Q., Zhu, Z., Li, C., Qin, Z., Sun, Q., 2016. Three dimensional seismic studies of deep-water hazard-related features on the northern slope of South China Sea. Mar. Pet. Geol. 77, 1125–1139.
Contreras-Rosales, L.A., Jennerjahn, T., Steinke, S., Mohtadi, M., Schefuß, E., 2019. Holocene changes in biome size and tropical cyclone activity around the Northern South China Sea. Quat. Sci. Rev. 215, 45–63.
Covault, J.A., Kostic, S., Paull, C.K., Ryan, H.F., Fildani, A., 2014. Submarine channel initiation, filling and maintenance from sea-floor geomorphology and morphodynamic modelling of cyclic steps. Sedimentology 61, 1031–1054.
Ercilla, G., Wynn, R.B., Alonso, B., Baraza, J., 2002. Initiation and evolution of turbidity current sediment waves in the Magdalena turbidite system. Mar. Geol. 192, 153–169.
García, M., Hernández-Molina, F.J., Llave, E., Stow, D.A.V., León, R., Fernández-Puga, M.C., Diaz del Río, V., Somoza, L., 2009. Contourite erosive features caused by the mediterranean outflow water in the gulf of cadiz: quaternary tectonic and oceanographic implications. Mar. Geol. 257, 24–40.
Gee, M.J.R., Gawthorpe, R.L., Bakke, K., Friedmann, S.J., 2007. Seismic geomorphology and evolution of submarine channels from the Angolan continental margin. J. Sediment. Res. 77, 433–446.
Georgiopoulou, A., Masson, D.G., Wynn, R.B., Krastel, S., 2010. Sahara Slide: age, initiation, and processes of a giant submarine slide. Geochem. Geophys. Geosyst. 11 (7), Q07014.
Gong, Z.S., Jin, Q., Qiu, Z., Wang, S., Meng, J., 1989. Geology tectonics and evolution of the Pearl River Mouth Basin. In: Zhu, X. (Ed.), Chinese Sedimentary Basins:

Amsterdam. Elsevier, Netherlands, pp. 181–196.
Gong, C., Wang, Y., Peng, X., Li, W., Qiu, Y., Xu, S., 2012. Sediment waves on the south China Sea slope off southwestern taiwan: implications for the intrusion of the northern pacific deep water into the south China sea. Mar. Pet. Geol. 32, 95–109.
Gong, C.L., Wang, Y.M., Zhu, W.L., Li, W.G., Xu, Q., 2013a. Upper Miocene to quaternary unidirectionally migrating deep-water channels in the Pearl River Mouth Basin, northern South China sea. AAPG Bull. 97, 285–308.
Gong, C., Wang, Y., Zhu, W., Li, W., Xu, Q., 2013b. Upper Miocene to quaternary unidirectionally migrating deep-water channels in the Pearl River Mouth Basin, northern South China sea. AAPG Bull. 97, 285–308.
Gong, C., Wang, Y., Xu, S., Pickering, K.T., Peng, X., Li, W., Yan, Q., 2015. The northeastern South China Sea margin created by the combined action of downslope and along-slope processes: processes, products and implications for exploration and paleoceanography. Mar. Pet. Geol. 64, 233–249.
Gong, C., Wang, Y., Rebesco, M., Salon, S., Steel, R.J., 2018. How do turbidity flows interact with contour currents in unidirectionally migrating deep-water channels? Geology 46, 551–554.
Haflidason, H., Sejrup, H.P., Nygård, A., Mienert, J., Bryn, P., Lien, R., Forsberg, C.F., Berg, K., Masson, D., 2004. The Storegga Slide: architecture, geometry and slide development. Mar. Geol. 213, 201–234.
He, Y., Xie, X., Kneller, B.C., Wang, Z., Li, X., 2013. Architecture and controlling factors of canyon fills on the shelf margin in the Qiongdongnan Basin, northern South China Sea. Mar. Pet. Geol. 41, 264–276.
He, Y., Zhong, G., Wang, L., Kuang, Z., 2014. Characteristics and occurrence of submarine canyon-associated landslides in the middle of the northern continental slope, South China Sea. Mar. Pet. Geol. 57, 546–560.
Hernández-Molina, F.J., Llave, E., Stow, D.A.V., García, M., Somoza, L., Vázquez, J.T., Lobo, F.J., Maestro, A., Díaz del Río, V., León, R., Medialdea, T., Gardner, J., 2006. The contourite depositional system of the Gulf of Cádiz: a sedimentary model related to the bottom current activity of the Mediterranean outflow water and its interaction with the continental margin. Deep Sea Res. Part II Top. Stud. Oceanogr. 53, 1420–1463.
Jobe, Z.R., Lowe, D.R., Uchytil, S.J., 2011. Two fundamentally different types of submarine canyons along the continental margin of Equatorial Guinea. Mar. Pet. Geol. 28, 843–860.
Laberg, J.S., Guidard, S., Mienert, J., Vorren, T.O., Haflidason, H., Nygård, A., 2007. Morphology and morphogenesis of a high-latitude canyon; the Andøya Canyon, Norwegian Sea. Mar. Geol. 246, 68–85.
Li, W., Wu, S.G., Völker, D., Zhao, F., Mi, L.J., Kopf, A., 2014. Morphology, seismic characterization and sediment dynamics of the Baiyun slide complex on the northern South China Sea margin. J. Geol. Soc. Lond. 171, 865–877.
Li, C.-F., Li, J., Ding, W., Franke, D., Yao, Y., Shi, H., Pang, X., Cao, Y., Lin, J., Kulhanek, D.K., Williams, T., Bao, R., Briais, A., Brown, E.A., Chen, Y., Clift, P.D., Colwell, F.S., Dadd, K.A., Hernández-Almeida, I., Huang, X.-L., Hyun, S., Jiang, T., Koppers, A.A.P., Li, Q., Liu, C., Liu, Q., Liu, Z., Nagai, R.H., Peleo-Alampay, A., Su, X., Sun, Z., Tejada, M.L.G., Trinh, H.S., Yeh, Y.-C., Zhang, C., Zhang, F., Zhang, G.-L., Zhao, X., 2015a. Seismic stratigraphy of the central South China Sea basin and implications for neotectonics. J. Geophys. Res.: Solid Earth 120, 1377–1399.
Li, W., Alves, T.M., Wu, S., Völker, D., Zhao, F., Mi, L., Kopf, A., 2015b. Recurrent slope failure and submarine channel incision as key factors controlling reservoir potential in the South China Sea (Qiongdongnan Basin, South Hainan Island). Mar. Pet. Geol. 64, 17–30.
Li, W., Krastel, S., Alves, T.M., Urlaub, M., Mehringer, L., Schürer, A., Feldens, P., Gross, F., Stevenson, C.J., Wynn, R.B., 2018. The agadir slide offshore NW africa: morphology, emplacement dynamics, and potential contribution to the Moroccan turbidite system. Earth Planet. Sci. Lett. 498, 436–449.
Lonergan, L., Jamin, N.H., Jackson, C.A.L., Johnson, H.D., 2013. U-shaped slope gully systems and sediment waves on the passive margin of Gabon (West Africa). Mar. Geol. 337, 80–97.
Lüdmann, T., Wong, H.K., Berglar, K., 2005. Upward flow of North Pacific deep water in the northern South China Sea as deduced from the occurrence of drift sediments. Geophys. Res. Lett. 32.
Ma, B., Wu, S., Sun, Q., Mi, L., Wang, Z., Tian, J., 2015. The late cenozoic deep-water channel system in the Baiyun sag, Pearl River Mouth Basin: development and tectonic effects. Deep Sea Res. Part II Top. Stud. Oceanogr. 122, 226–239.
Martorelli, E., Bosman, A., Casalbore, D., Chiocci, F.L., Falcini, F., 2016. Interaction of down-slope and along-slope processes off Capo Vaticano (southern Tyrrhenian Sea, Italy), with particular reference on contourite-related landslides. Mar. Geol. 378, 43–55.
Micallef, A., Mountjoy, J.J., 2011. A topographic signature of a hydrodynamic origin for submarine gullies. Geology 39, 115–118.
Moscardelli, L., Wood, L., Mann, P., 2006. Mass-transport complexes and associated processes in the offshore area of Trinidad and Venezuela. AAPG (Am. Assoc. Pet. Geol.) Bull. 90, 1059–1088.
Mosher, D.C., Campbell, D.C., Gardner, J.V., Piper, D.J.W., Chaytor, J.D., Rebesco, M., 2017. The role of deep-water sedimentary processes in shaping a continental margin: the Northwest Atlantic. Mar. Geol. 393, 245–259.
Normark, W.R., Piper, D.J.W., Posamentier, H., Pirmez, C., Migeon, S., 2002. Variability in form and growth of sediment waves on turbidite channel levees. Mar. Geol. 192, 23–58.
Perez-Hernandez, S., Comas, M.C., Escutia, C., 2014. Morphology of turbidite systems within an active continental margin (the Palomares Margin, western Mediterranean). Geomorphology 219, 10–26.
Pubellier, M., Ego, F., Chamot-Rooke, N., Rangin, C., 2003. The building of pericratonic mountain ranges: structural and kinematic constraints applied to GIS-based reconstructions of SE Asia. Bull. de la Société géologique de France 174 (6), 561–584.
Qin, Y., Alves, T., Constantine, J.A., Gamboa, D., 2017. The role of mass wasting in the progressive developmentof submarine channels (Espırito Santo Basin, SE Brazil). J. Sediment. Res. 87, 500–516.
Rebesco, M., Pudsey, C.J., Canals, M., Camerlenghi, A., Barker, P.F., Estrada, F., Giorgetti, A., 2002. Sediment drifts and deep-sea channel systems. Antarctic Peninsula Pacific Margin, vol. 22. Geological Society, London, pp. 353 Memoir.
Rasmussen, S., Lykke-Andersen, H., Kuijpers, A., Troelstra, S.R., 2003. Post-Miocene sedimentation at the continental rise of Southeast Greenland: the interplay between turbidity and contour currents. Mar. Geol. 196, 37–52.
Rebesco, M., Camerlenghi, A., Volpi, V., Neagu, C., Accettella, D., Lindberg, B., Cova, A., Zgur, F., 2007. Interaction of processes and importance of contourites: insights from the detailed morphology of sediment Drift 7, Antarctica. Geological Society, London, Special Publications 276, 95.
Rebesco, M., Wåhlin, A., Laberg, J.S., Schauer, U., Beszczynska-Möller, A., Lucchi, R.G., Noormets, R., Accettella, D., Zarayskaya, Y., Diviacco, P., 2013. Quaternary contourite drifts of the Western Spitsbergen margin. Deep Sea Res. Oceanogr. Res. Pap. 79, 156–168.
Rebesco, M., Hernández-Molina, F.J., Van Rooij, D., Wåhlin, A., 2014. Contourites and associated sediments controlled by deep-water circulation processes: state-of-the-art and future considerations. Mar. Geol. 352, 111–154.
Rebesco, M., Özmaral, A., Urgeles, R., Accettella, D., Lucchi, R.G., Rüther, D., Winsborrow, M., Llopart, J., Caburlotto, A., Lantzsch, H., Hanebuth, T.J.J., 2016. Evolution of a high-latitude sediment drift inside a glacially-carved trough based on high-resolution seismic stratigraphy (Kveithola, NW Barents Sea). Quat. Sci. Rev. 147, 178–193.
Shepard, F.P., 1936. The underlying causes of submarine canyons. Proc. Natl. Acad. Sci. U.S.A. 22 (8), 496–502.
Shepard, F.P., 1981. Submarine canyons; multiple causes and long-time persistence. Am. Assoc. Petrol. Geol. Bull. 65, 1062–1077.
Steinke, S., Kienast, M., Hanebuth, T., 2003. On the significance of sea-level variations and shelf paleo-morphology in governing sedimentation in the southern South China Sea during the last deglaciation. Mar. Geol. 201, 179–206.
Steinke, S., Chiu, H.-Y., Yu, P.-S., Shen, C.-C., Erlenkeuser, H., Löwemark, L., Chen, M.-T., 2006. On the influence of sea level and monsoon climate on the southern South China Sea freshwater budget over the last 22,000 years. Quat. Sci. Rev. 25, 1475–1488.
Steinke, S., Groeneveld, J., Johnstone, H., Rendle-Bühring, R., 2010. East Asian summer monsoon weakening after 7.5Ma: evidence from combined planktonic foraminifera Mg/Ca and δ18O (ODP Site 1146; northern South China Sea). Palaeogeogr. Palaeoclimatol. Palaeoecol. 289, 33–43.
Sun, Q., Xie, X., Piper, D.J.W., Wu, J., Wu, S., 2017. Three dimensional seismic anatomy of multi-stage mass transport deposits in the Pearl River Mouth Basin, northern South China Sea: their ages and kinematics. Mar. Geol. 393, 93–108.
Sun, Q., Alves, T.M., Lu, X., Chen, C., Xie, X., 2018a. True volumes of slope failure estimated from a quaternary mass-transport deposit in the northern South China sea. Geophys. Res. Lett. 45 (6), 2642–2651.
Sun, Q., Cartwright, J., Xie, X., Lu, X., Yuan, S., Chen, C., 2018b. Reconstruction of repeated Quaternary slope failures in the northern South China Sea. Mar. Geol. 401, 17–35.
Surlyk, F., Lykke-Andersen, H., 2007. Contourite drifts, moats and channels in the Upper Cretaceous chalk of the Danish Basin. Sedimentology 54, 405–422.
Tian, J., Yang, Q., Liang, X., Xie, L., Hu, D., Wang, F., Qu, T., 2006. Observation of Luzon Strait transport. Geophys. Res. Lett. 33, L19607.
Vandorpe, T., Martins, I., Vitorino, J., Hebbeln, D., García, M., Van Rooij, D., 2016. Bottom currents and their influence on the sedimentation pattern in the El Arraiche mud volcano province, southern Gulf of Cadiz. Mar. Geol. 378, 114–126.
Vorren, T.O., Laberg, J.S., Blaume, F., Dowdeswell, J.A., Kenyon, N.H., Mienert, J., Rumohr, J.A.N., Werner, F., 1998. The Norwegian–Greenland Sea continental margins: morphology and Late Quaternary sedimentary processes and environment. Quat. Sci. Rev. 17, 273–302.
Wang, X., Wang, Y., He, M., Chen, W., Zhuo, H., Gao, S., Wang, M., Zhou, J., 2017. Genesis and evolution of the mass transport deposits in the middle segment of the Pearl River canyon, South China Sea: insights from 3D seismic data. Mar. Pet. Geol. 88, 555–574.
Wang, X., Zhuo, H., Wang, Y., Mao, P., He, M., Chen, W., Zhou, J., Gao, S., Wang, M., 2018. Controls of contour currents on intra-canyon mixed sedimentary processes: insights from the Pearl River Canyon, northern South China Sea. Mar. Geol. 406, 193–213.
Wu, S., Gao, J., Zhao, S., Lüdmann, T., Chen, D., Spence, G., 2014. Post-rift uplift and focused fluid flow in the passive margin of northern South China Sea. Tectonophysics 615–616, 27–39.
Wynn, R.B., Stow, D.A.V., 2002. Classification and characterisation of deep-water sediment waves. Mar. Geol. 192, 7–22.
Xie, X., Müller, R.D., Li, S., Gong, Z., Steinberger, B., 2006. Origin of anomalous subsidence along the Northern South China Sea margin and its relationship to dynamic topography. Mar. Pet. Geol. 23, 745–765.
Zhao, W., Zhou, C., Tian, J.W., Yang, Q.X., Wang, B., Xie, L.L., Qu, T.D., 2014. Deep water circulation in the Luzon Strait. J. Geophys. Res. Oceans 119, 790–804.
Zhao, F., Alves, T.M., Li, W., Wu, S., 2015. Recurrent slope failure enhancing source rock burial depth and seal unit competence in the Pearl River Mouth Basin, offshore South China Sea. Tectonophysics 643, 1–7.
Zhao, F., Alves, T.M., Wu, S., Li, W., Huuse, M., Mi, L., Sun, Q., Ma, B., 2016. Prolonged post-rift magmatism on highly extended crust of divergent continental margins (Baiyun Sag, South China Sea). Earth Planet. Sci. Lett. 445, 79–91.
Zhu, M., Graham, S., Pang, X., McHargue, T., 2010. Characteristics of migrating submarine canyons from the middle Miocene to present: implications for paleoceanographic circulation, northern South China Sea. Mar. Pet. Geol. 27, 307–319.